ACTA ABP BIOCHIMICA POLONICA

Vol. 70, No 3/2023
525–532
https://doi.org/10.18388/abp.2020_6459

Regular paper

Circ_PWWP2A promotes lung fibroblast proliferation and fibrosis *via* the miR-27b-3p/GATA3 axis, thereby aggravating idiopathic pulmonary fibrosis

LiQing Su[1#], Ying Nian[1#] and TianJi Zhu[1]✉

Department of Respiratory and Critical Care Medicine, Affiliated Hospital of Inner Mongolia Medical University, Hohhot City, Inner Mongolia Autonomous Region, 010050, China

Objective: This paper was to investigate the effect of circ_PWWP2A-mediated miR-27b-3p/GATA3 axis on idiopathic pulmonary fibrosis (IPF). Methods: circ_PWWP2A expression in lung fibroblasts MLg2908 induced by different concentrations of TGF-β was detected. The relationship between circ_PWWP2A or GATA3 and miR-27b-3p was analyzed by RNA immunoprecipitation and dual-luciferin reporter assay. The proliferation of MLg2908 cells was determined by MTT. GATA3, α-SMA, Collagen-I, and Collagen-III in cells were detected by RT-qPCR and Western blot. The rat model of IPF induced by bleomycin (BLM) was constructed and treated with circ_PWWP2A siRNA injection. HE and Masson staining were of utility to evaluate the pathological conditions of rat lung tissue, and circ_PWWP2A, miR-27b-3p, and GATA3 levels in lung tissues were detected by RT-qPCR. Immunohistochemistry was used to detect the staining of α-SMA, collagen I, and collagen III in the lung tissues of rats. Results: circ_PWWP2A in MLg2908 cells induced by TGF-β decreased in a concentration-dependent manner. MLg2908 cells transfected with circ_PWWP2A siRNA were induced by 5 ng/ml TGF-β, decreasing circ_PWWP2A and GATA3 levels, increasing miR-27b-3p expression, and suppressing cell proliferation. The targeting relationship between circ_PWWP2A and miR-27b-3p, as well as miR-27b-3p and GATA3, was confirmed. Depleting miR-27b-3p reduced the inhibitory effect of circ_PWWP2A down-regulation on the proliferation of TGF-β-treated MLg2908 cells, accompanied by increased expression of α-SMA, Collagen 1, and Collagen 3, and increased expression of GATA3. The *in vivo* results showed that BLM-induced fibrosis in rat lung tissue was obvious, accompanied by increased expression of circ_PWWP2A and GATA3, decreased expression of miR-27b-3p, and deepened staining of α-SMA, collagen I, and collagen III, but circ_PWWP2A siRNA could improve these phenomena. Conclusion: Silencing circ_PWWP2A can inhibit the proliferation of lung fibroblasts induced by TGF-β through the miR-27b-3p/GATA3 axis, and reduce BLM-induced pulmonary fibrosis in rats, which may be a potential therapeutic target for IPF.

Keywords: Lung fibroblasts, circ_PWWP2A, miR-27b-3p, GATA3, Idiopathic pulmonary fibrosis

Received: 10 August, 2022; revised: 25 May, 2023; accepted: 29 May, 2023; available on-line: 06 September, 2023

✉e-mail: hutianjinmg@hotmail.com
#These authors contributed equally to this work
Abbreviations: circRNA, Circular RNA; IPF, Idiopathic pulmonary fibrosis

INTRODUCTION

Idiopathic pulmonary fibrosis (IPF) is a diffuse parenehymal lung disease, which is a group of interstitial lung diseases (Martinez *et al.*, 2017; Xaubet *et al.*, 2017). IPF is a representative interstitial lung disease (Sgalla *et al.*, 2016) that is pathologically featured by diffuse alveolitis, pulmonary fibrosis, and progressive scarring. The clinical manifestations are mainly no obvious cause, and the initial symptoms are exertional dyspnea and chronic cough without sputum (Konigsberg *et al.*, 2021; Wolters *et al.*, 2014).

At present, there are mainly anti-inflammatory drugs (such as prednisone) for inflammation, and immunosuppressants (such as cyclophosphamide) for immune response. However, the application of these two types of drugs can affect the inflammatory response of IPF, but not improve the progress of immune response and immune response much, or increase the survival rate of patients (Hewlett *et al.*, 2018; Somogyi *et al.*, 2019). These include nintedanib (Ofev®) and pirfenidone (Esbriet®). These medications are called anti-fibrotic agents, Nintedanib inhibits inflammation and fibrosis by blocking a variety of tyrosine kinase receptors, including platelet-derived growth factor, vascular endothelial growth factor, and fibroblast growth factor (Hilberg *et al.*, 2008). The main antifibrotic effect of pirfenidone is to down-regulate transforming growth factor-β (Nakayama *et al.*, 2008). Such as Tananchai et al data confirm that multicenter phase III randomized controlled trial of pirfenidone and niintedanib (ASCEND and INPULSIS Q7) showed a similar reduction in lung function decline compared with placebo (King *et al.*, 2014).The long-term effects of antifibrotic therapy on mortality are unknown. Real-world and registry-based studies have been published describing the long-term use of antifibrotic drugs in clinical practice (Nathan *et al.*, 2017). These studies showed that about 40 percent of patients had drug-related adverse effects, including diarrhea, gastrointestinal distress, and elevated transaminases. However, only 5% of patients receiving antifibrotic therapy permanently discontinue treatment(Cerri *et al.*, 2019). Such studies also add to the growing number of reports on the long-term efficacy of antifibrotic drugs.Therefore, IPF has a poor prognosis and a high mortality rate (Wakwaya & Brown, 2019). IPF generally affects men after the age of 60 years and a median survival time of 2–4 years, even worse than many cancers (Vancheri *et al.*, 2010; Sgalla *et al.*, 2016). It was reported that the survival rate is as low as 2–5 years after diagnosis of the IPF(Richeldi *et*

al., 2017).Therefore, how to prevent and treat IPF more effectively is a difficult problem faced by clinicians.

Circular RNA (circRNA) closed circular RNA molecules formed by covalent bonds (Kristensen *et al*., 2019). Studies have proved that circRNAs exerts a regulatory role in eukaryotic life activities and disease developments, such as cardiovascular diseases (Altesha *et al*., 2019), tumors (Lei *et al*., 2020; Li *et al*., 2020), kidney-related diseases (Jin *et al*., 2020), and lung-related diseases (M. *et al*., 2020), including IPF (Li *et al*., 2018). For example, hsa_circ_0058493 knockdown inhibits fibrosis by affecting the epithelial-mesenchymal transition (EMT) process in IPF (Cheng *et al*., 2022). Has_circ_PWWP2A, also known as hsa_circ_0074837 (Zhang *et al*., 2018), was found to be associated with promoting liver fibrosis (Liu *et al*., 2019). A reliable function of circRNAs is to directly or indirectly bind target miRNAs to inhibit miRNA function through a process commonly referred to as miRNA sponge adsorption (Huang *et al*., 2020). Through ENCORI comprehensive database, we found that circ_PWWP2A has a potential binding site with miR-27b-3p. miR-27b-3p has been discovered to be correlated with renal fibrosis (Conserva *et al*., 2019). Microarray analysis revealed that downregulation of miR-27b-3p is associated with fibrosis (Kim *et al*., 2017). Furthermore, miR-27b-3p expression alters significantly during lung exacerbation in cystic fibrosis patients (Stachowiak *et al*., 2020).

Therefore, this article targeted to reveal the mechanism related to circ_PWWP2A and the regulatory network of circ_PWWP2A/miR-27b-3p/GATA3 in IPF, with the purpose to develop molecule-based therapy.

MATERIALS AND METHODS

Cell culture and treatment

The murine lung fibroblast cell line MLg2908 (ATCC, CCL-206, USA) was maintained in EMEM (30-2003, ATCC, USA) containing 10% FBS and treated with different concentrations of recombinant human TGF-β (10 ng/ml; PeproTech, USA; 0, 5, 10 ng/ml) for 24 h (Y. J. Li et al., 2006). circ_PWWP2A siRNA#1, circ_PWWP2A siRNA#2, and NC siRNA were transfected in MLg2908 cells according to Lipofectamine 3000 reagent (L3000001, Thermo Fisher Scientific), and the more effective siRNA was selected for later experiments. MLg2908 were treated with TGF-β at an optimal concentration of 5 ng/ml for 24 h. Before induction, Cells were cultured in 6-well plates with a concentration of 4×105 cells/well, the cells were transfected with the following plasmids, including circ_PWWP2A siRNA#2 and miR-27b-3p inhibitors (#AM17000, Thermo Fisher Scientific).Cells were incubated with 2 ml Opti-MEM medium (GIBCO, USA) containing plasmids (1 μg) and Lipofectamine 3000 (2.5 μl). The medium was changed after 6 h, and the RNA extraction was performed at 48 h to verify the transfection efficiency.

RNA immunoprecipitation (RIP)

Protein-A/G-coated magnetic beads were resuspended in 100 μl NT-2 buffer and let stand with 5 μg AGO2-labeled antibody(Millipore, Billerica, MA, USA). Cells were centrifuged, and 100 μl of the supernatant was added to 900 μl of magnetic beads resuspended in NET-2 buffer. Appropriate antisense probes were designed according to the unique trans-cleavage site of circRNA, and the corresponding sense sequences were used as control negative probes. Briefly, cells were lysed in RIP lysis buffer, then supernatants were transferred to nuclease-free tubes, magnetic beads conjugated to Ago2 or IgG antibodies were added and incubated for 6 hours at 4°C. The immunoprecipitates bound to the beads were eluted with elution buffer, and the purified RNA fragments were analyzed by RT-qPCR.

MTT experiment

Cells were taken after trypsinization and centrifuged to prepare a cell suspension at 5×10^4 cells/mL. Seeded into 96-well plates to 45 Wells, 200 μL of cell suspension was cultured for 24 h and centrifuged at 1000 r/min (supernatant was removed). Afterward, 200 μL of serum-free culture medium and 20 μL of 5 mg/ml MTT were added to each well for an additional 4 h, centrifuged at 1000 rpm/min (supernatant was removed), and reacted with 200 μL DMSO to record OD_{490} value on a microplate reader.

Luciferase activity assay

Bioinformatics software predicted the binding sites of circ_PWWP2A and miR-27b-3p, as well as miR-27b-3p and GATA3, and a miR-27b-3p recombinant firefly luciferase reporter plasmid containing the circ_PWWP2A/GATA3 binding sequence was designed and synthesized. circ_PWWP2A WT/circ_PWWP2A MUT/GATA3 WT/GATA3 MUT was co-transfected with mimic NC or miR-27b-3p mimics into MLg2908, respectively. After 48 h, the luciferase activity of the cells was detected according to the instructions of the Dual-Luciferase reporter system kit (Promega).

Immunoblot analysis

Proteins were extracted by lysing cells with RIPA buffer (Sigma, USA) containing protease inhibitors and subsequently quantified by a BCA protein concentration assay kit(Beyotime Biotechnology, Nanjing, China). Total protein was loaded onto PVDF membrane (ThermoFisher Scientific, USA) after 10% SDS-PAGE gel electrophoresis, then blocked with 5% nonfat milk powder, and with primary antibodies at 4°C overnight, including α-SMA at 1 μg/ml (ab5694, Abcam), collagen I (1:5000, ab260043, Abcam), collagen III (1:5000, ab7778, Abcam), GATA3 (1:1000, ab199428, Abcam) and GAPDH (1:2500, ab9548, Abcam). The next day, secondary antibodies were added and incubated for 40 min, the membrane interacted with HRP-conjugated goat anti-rabbit IgG secondary antibody (#31460, Thermo Fisher Scientific). Immunoblots were visualized in IBright FL1500 Intelligent Imaging System (ThermoFisher, USA) and GAPDH was used as an internal control.

Establishment and treatment of IPF rat model

Twenty-four SD male rats, weighing about 200 g, were treated accordingly (6 rats in each group). The rats were anesthetized by intraperitoneal 10% chloral hydrate and fixed in a supine position to expose the trachea. After anesthesia, 1 mg BLM was added to 0.5 ml PBS for intratracheal administration (Otsuka *et al*., 2017), while the Sham group was only given 0.5 ml PBS. Fourteen days after modeling (day 15), 1 μl/g siRNA was intravenously injected into rats at 0.75 mg/kg/day, three times every other day. Twenty-four hours after the last injection, rats were euthanized by pentobarbital sodium, and lungs were harvested for HE staining and Masson stain-

Table 1. Primer sequences for PCR

Genes	Sequence (5′-3′)	
	Forward	Reverse
circ_PWWP2A	AAGACAGGACTTGAGAAAATGC	GGCATGGCTTCTGGTTTATC
miR-27b-3p	AGTGGCTAAGTTCTGCCTCAAC	CTCAACTGGTGTCGTGGAGTC
GATA3	AAGCTCAGTATCCGCTGACG	GTTTCCGTAGTAGGACGGGAC
α-SMA	CCCAGACATCAGGGAGTAATGG	TCTATCGGATACTTCAGCGTCA
collagen I	GCTCCTCTTAGGGGCCACT	ATTGGGGACCCTTAGGCCAT
collagen III	CTGTAACATGGAAACTGGGGAAA	CCATAGCTGAACTGAAAACCACC
U6	GATTCGGACGTTGTATCGCTG	CTCGGAGTTGCACCAAATCC
GAPDH	TGGATTTGGACGCATTGGTC	TTTGCACTGGTACGTGTTGAT

Note: circ_PWWP2A, circular RNA PWWP2A; miR-27b-3p, microRNA-27b-3p; GATA3, GATA Binding Protein-3; α-SMA, α-smooth muscle actin; GAPDH, glyceraldehyde-3-phosphate dehydrogenase.

ing (Milara *et al*., 2018; Otsuka *et al*., 2017). Fibrosis was scored according to the Ashcroft assay.

Immunohistochemistry

Fresh paraffin tissues (4 μm) were placed in an oven at 65°C for 2 h, deparaffinized to water, and microwaved in EDTA buffer. Sections were placed in 3% hydrogen peroxide solution for 10 min, blocked with 5% BSA for 20 min, added about 50 μl of diluted primary antibody overnightincluding α-SMA at 1 μg/ml (ab5694, Abcam), collagen I (1:5000, ab260043, Abcam), collagen III (1:5000, ab7778, Abcam), GATA3 (1:1000, ab199428, Abcam) and GAPDH (1:2500, ab9548, Abcam), and 50-100 μl secondary antibody for 50 minthe (membrane interacted with HRP-conjugated goat anti-rabbit IgG secondary antibody (#31460, Thermo Fisher Scientific). After the addition of DAB solution, the sections were counterstained with hematoxylin, differentiated with 1% hydrochloric acid alcohol, immersed in ammonia, dehydrated with gradient alcohol, cleared with xylene, and mounted with neutral gum.

RT-qPCR

Cell and tissue RNA was extracted by the Trizol method, and the concentration and quality of the RNA solution were determined on a DU730 instrument. RNA was reverse transcribed into cDNA using SuperScript IV Reverse Transcriptase (#18090010, Invitrogen) and treated with qPCR according to the SuperScript III Platinum SYBR Green One-Step qRT-PCR Kit (#11736059, Invitrogen). The primer sequences are shown in Table 1. Transcription level of the target gene was calculated by $2^{-\Delta\Delta Ct}$ method.

Statistical analysis

SPSS 19.0 software was of utility for statistical analysis and Graphpad 6.0 was for drawing graphs. One-way analysis of variance, along with Tukey's HSD test was suitable for assessing data collected from multiple groups. Differences were considered statistically significant at $P<0.05$.

RESULTS

circ_PWWP2A can affect the proliferation of TGF-β-treated MLg2908

To investigate the function of circ_PWWP2A in MLg2908 cells, we first knocked it down by transforming the cells using two lentiviral vectors encoding independent shRNAs targeting circ_PWWP2A.

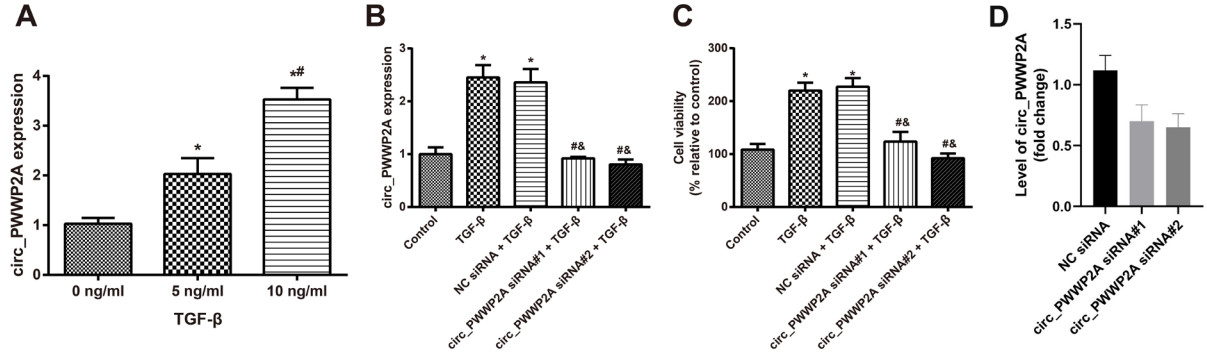

Figure 1. circ_PWWP2A can inhibit the proliferation of mouse lung fibroblasts treated with TGF-β
(**A**) circ_PWWP2A expression after MLg2908 cells were treated with different concentrations of TGF-β (0, 5, 10 ng/ml), *vs. 0 ng/ml TGF-β, $P<0.05$; #vs. 5 ng/ml TGF-β, $P<0.05$; (**B**) circ_PWWP2A expression in MLg2908 cells co-treated with circ_PWWP2A siRNA and 5 ng/ml TGF-β; (**C**) Proliferation of MLg2908 cells after co-treatment with circ_PWWP2A siRNA and 5 ng/ml TGF-β; *vs. Control group, $P<0.05$; #vs. TGF-β group and NC siRNA + TGF-β group, $P<0.05$; &vs. circ_PWWP2A siRNA + TGF-β group, $P<0.05$. (**D**) qRT-PCR analysis of circ_PWWP2A levels in MLg2908 cells infected with a lentiviral vector encoding circ_PWWP2A siRNA#1 or circ_PWWP2A siRNA#2

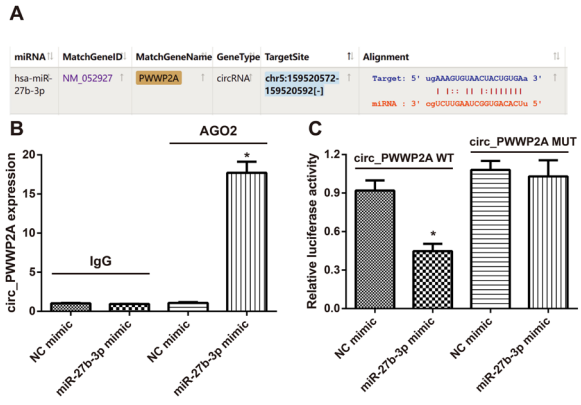

Figure 2. circ_PWWP2A can adsorb miR-27b-3p
(**A**) ENCORI found that circ_PWWP2A and miR-27b-3p have potential binding sites; (**B**) RIP to further verify the interaction relationship between circ_PWWP2A and miR-27b-3p; (**C**) dual luciferase reporter experiment to verify the targeting relationship between circ_PWWP2A and miR-27b-3p; *vs. other three groups, $P<0.05$.

RT-qPCR analysis confirmed that circ_PWWP2A levels were suppressed to a greater degree by expression of circ_PWWP2A (Fig. 1D), which was then utilized in subsequent experiments. In MLg2908 cells treated with different concentrations of TGF-β (0, 5, 10 ng/ml), circ_PWWP2A was increased in a concentration-dependent manner (Fig. 1A), indicating that circ_PWWP2A is promoted during lung fibroblast activation. MLg2908 cells were transfected with circ_PWWP2A siRNA and then induced by 5 ng/ml TGF-β, and it was found that circ_PWWP2A in the cells was decreased (Fig. 1B), After 48 h of TGF-β treatment accompanied by a decrease in prsoliferation activity (Fig. 1C). It indicated that the low expression of circ_PWWP2A could inhibit the proliferation of lung fibroblasts induced by TGF-β.

circ_PWWP2A can adsorb miR-27b-3p

Bioinformatics analysis ENCORI found that circ_PWWP2A has a potential binding site with miR-27b-3p (Fig. 2A). Next, RIP assays in MLg2908 cells further verified the interaction between circ_PWWP2A and miR-27b-3p. circ_PWWP2A was richly precipitated with anti-AGO2 after overexpressing miR-27b-3p in cells (Fig. 2B). Dual-luciferase reporter gene assay results showed that miR-27b-3p can reduce the luciferase activity of circ_PWWP2A WT (Fig. 2C) but not circ_PWWP2A MUT, indicating that circ_PWWP2A has a direct interaction with miR-27b-3p.

Consumpting miR-27b-3p enhances the proliferation of TGF-β-induced MLg2908 cells

Figure 3A showed that 5 ng/ml TGF-β can inhibit miR-27b-3p expression in MLg2908 cells, and after co-treatment with miR-27b-3p inhibitors, miR-27b-3p expression was further reduced, and the accompanying cell proliferation was further activated. circ_PWWP2A siRNA could reduce TGF-β-regulated inhibition of miR-27b-3p, that is, circ_PWWP2A siRNA augmented miR-27b-3p expression in TGF-β-treated MLg2908 cells.

Silencing miR-27b-3p affects fibrosis-related genes in lung fibroblasts

α-SMA, collagen I, and collagen III in cells were determined by RT-qPCR and immunoblot analysis (Fig. 4A, B), demonstrating an increase α-SMA, collagen I, and collagen III increased in MLg2908 after TGF-β induction, which was promoted α-SMA, collagen I, and collagen III express after co-treatment with miR-27b-3p inhibitors, but alleviated α-SMA, collagen I, and collagen express III after circ_PWWP2A siRNA co-treatment. miR-27b-3p inhibitor co-treatment lessened circ_PWWP2A siRNA-regulated suppression of these fibrosis-related genes.

circ_PWWP2A can regulate GATA3 expression through miR-27b-3p

ENCORI database showed that GATA3 was a direct target gene of miR-27b-3p (Fig. 5A). The interaction between the two was further verified by luciferase experiments, as the results showed that miR-27b-3p mimic reduced the luciferase activity of GATA3 WT without affecting that of GATA3 MUT (Fig. 5B). Our test results also found that circ_PWWP2A siRNA could inhibit the increase of GATA3 in MLg2908 cells induced by TGF-β, while miR-27b-3p inhibitors did oppositely. GATA3 was down-regulated in MLg2908 cells co-treated with TGF-β and circ_PWWP2A siRNA, but this phenomenon was reversed by miR-27b-3p inhibitors (Fig. 5C–E).

Therapeutic effect of circ_PWWP2A siRNA on IPF rats

HE staining and Masson staining showed (Fig. 6A): in rats receiving sham operation, lung structure was normal, the alveolar interval was uniform, no obvious exudation was seen in the cavity, and a small number of collagen fibers dyed in light blue can be seen in the alveoli, but without obvious pathological change. However, BLM injection destroyed the alveolar structure, reduced the alveolar cavity, exfoliated alveolar epithelium and protein exudate, and caused obvious collagen deposition and fibrosis areas. circ_PWWP2A siRNA-treated rats consti-

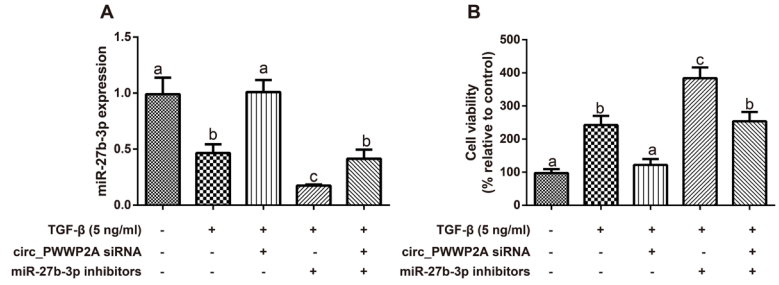

Figure 3. Depleting miR-27b-3p enhances the proliferation of TGF-β-induced MLg2908 cells
(**A**) miR-27b-3p expression in MLg2908 cells; (**B**) Proliferation of MLg2908 cells; the same letter indicates no statistical significance, $P>0.05$; different letters indicate statistical differences, $P<0.05$.

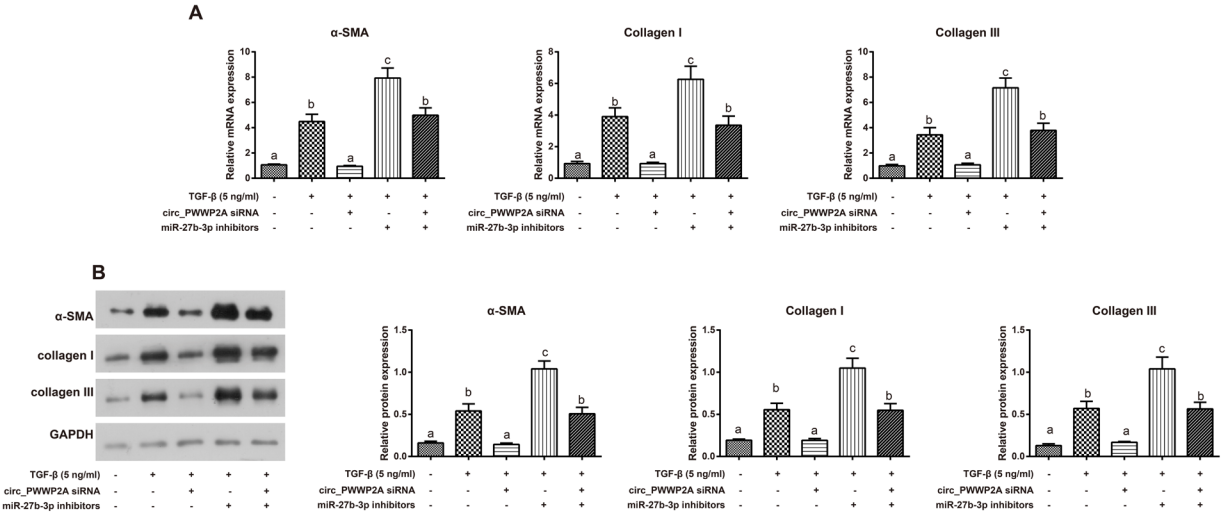

Figure 4. Silencing miR-27b-3p affects fibrosis-related genes in lung fibroblasts
(**A**) qRT-PCR analysis α-SMA, collagen I, and collagen III in MLg2908 cells (Three technical replicates and three biological replicates); the same letter indicates no statistical significance, $P>0.05$; different letters indicate statistical differences, $P<0.05$. (**B**) WB analysis α-SMA, collagen I, and collagen III in MLg2908 cells (Three technical replicates and three biological replicates); the same letter indicates no statistical significance, $P>0.05$; different letters indicate statistical differences, $P<0.05$.

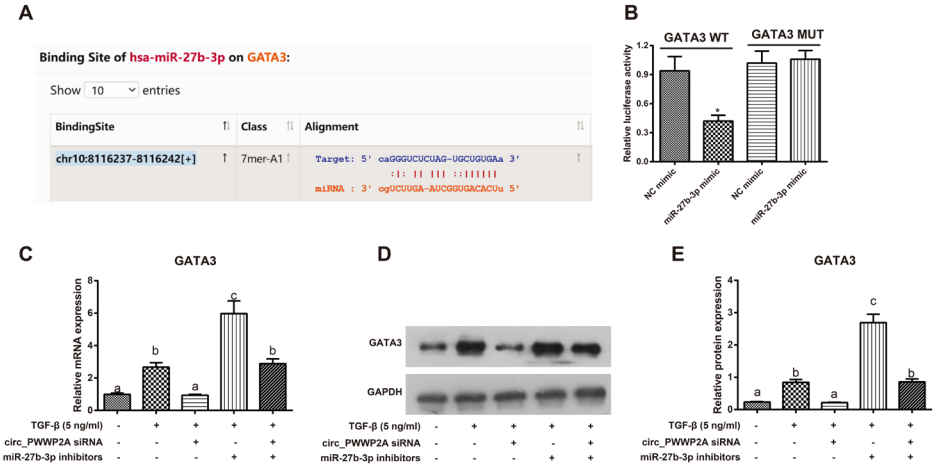

Figure 5. circ_PWWP2A can regulate GATA3 expression through miR-27b-3p
(**A**) ENCORI showed that GATA3 is a direct target gene of miR-27b-3p; (**B**) Dual luciferase reporter experiment verified the targeting relationship between GATA3 and miR-27b-3p, *vs. other three groups, $P<0.05$; (**C–E**) GATA3 expression in cells; the same letter indicates no statistical significance, $P>0.05$; different letters indicate statistical differences, $P<0.05$.

tuted mild hyperplasia of fibroblasts, deposition of collagen fibers in the pleura and alveolar septa, and mild to moderate pulmonary fibrosis. Ashcroft scores indicated that BLM-induced rats had higher Ashcroft scores, but circ_PWWP2A siRNA reduced Ashcroft scores in BLM-treated rats (Fig. 6B). BLM-induced increased expression of circ_PWWP2A and GATA3 in rat lung tissue, while decreased expression of miR-27b-3p, was reversed by circ_PWWP2A siRNA treatment (Fig. 6C). BLM rats had enhanced immunohistochemical staining results of α-SMA, collagen I and collagen III in lung tissue, but the staining degree was reduced after circ_PWWP2A siRNA injection (Fig. 6D).

DISCUSSION

In humans, IPF is a progressive disease associated with aging caused by uncontrolled proliferation and differentiation of fibroblasts resulting from sustained damage to the alveolar epithelium.These myofibroblasts are responsible for hyperproliferation, EMT, ECM production, and contribute to collagen deposition in the affected organ (King *et al.*, 2011). Transforming growth factor-β1 (TGF-β1) is a key member of the TGF-β superfamily. It was discovered in 1983 for its ability to stimulate the growth of rat fibroblasts cultured in soft AGAR and has been identified as a master cytokine in liver fibrosis (Xu *et al.*, 2016).In fibrosis, increased TGF-β signaling significantly affects the behavior of the fibroblast population, which represents the majority of cells in fibrotic lesions. In addition, low levels of TGF-β promoted fibroblast proliferation (Zhang *et al.*, 2017). These activities may explain the number of fibroblasts in fibrotic lesions.Tgf-β-induced mesenchymal characteristics enable epithelial and endothelial cells to contribute to fibroblast popula-

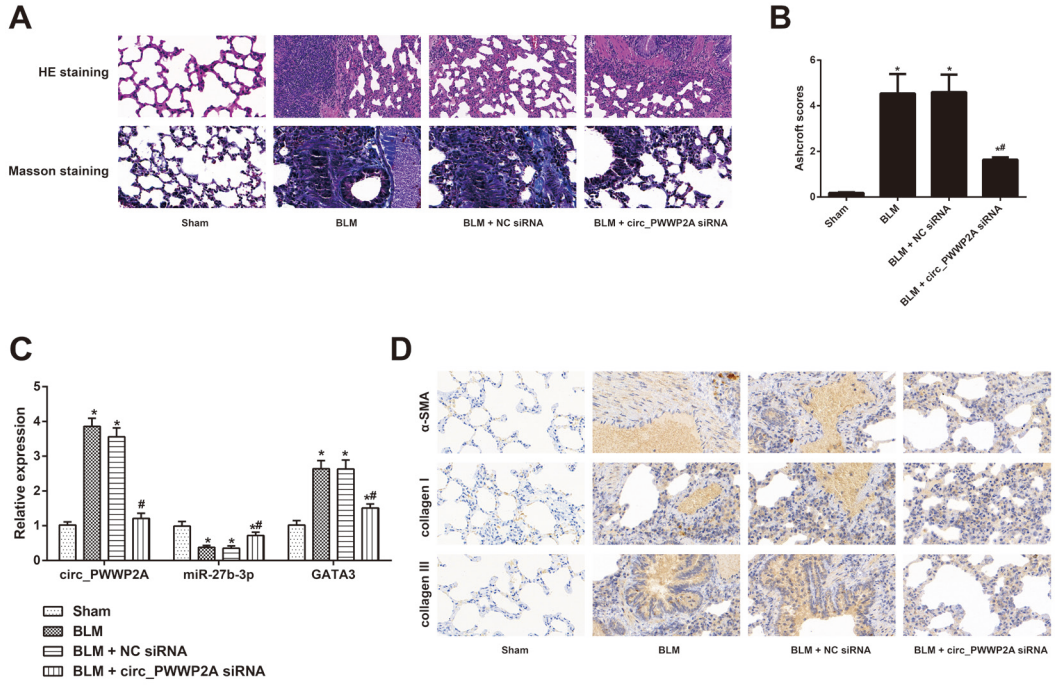

Figure 6. Therapeutic effect of circ_PWWP2A siRNA on IPF rats
(**A**) HE staining and Masson staining of lung tissue; (**B**) Ashcroft scores in lung tissue; (**C**) circ_PWWP2A, miR-27b-3p and GATA3 expression in lung tissue; (**D**) Immunohistochemical detection of α-SMA, collagen I, and collagen III staining in lung tissue.

tion in fibrotic diseases, which has been revealed in a mouse model of fibrosis (Katsuno *et al*., 2021).

With the rapid development of deep transcriptome sequencing technology, the research on noncoding RNAs is growing exponentially(Matsui *et al*., 2017),Although in some cases ncrnas lack protein-coding capabilities and appear to lack biological functions, increasing evidence confirms that they play a critical role in controlling gene expression through multiple mechanisms, such as targeting transcripts (Liu *et al*., 2012). Reports have demonstrated that several lncRNAs and miRNAs play critical roles in the progression of IPF. For instance, Li and others (Li *et al*., 2020) reported that circTADA2A could repress fibroblasts activation and proliferation *via* miR-526b/Cav1 and miR-203/Cav2 pathway, thus alleviating IPF. Anotherhsa_circ_0044226 was markedly higher in lung tissues from IPF patients than from healthy controls. which RLE-6TN cells and in a bleomycin-induced mouse model of IPA and diminished TGF-β1-induced fibrosis.these findings indicate that downregulation of hsa_circ_0044226 attenuates pulmonary fibrosis in vitro and in vivo by inhibiting CDC27, which in turn suppresses EMT. This suggests hsa_circ_0044226 may be a useful therapeutic target for the treatment of IPF (Qi *et al*., 2020). In addition, lncRNA H19 (Lu *et al*., 2018), MEG3 (Gokey *et al*., 2018) have been also confirmed to paly critical roles in IPF.

At present, previous studies have found that circ_PWWP2A plays a role in various diseases. For example, in OB-6 osteoblasts and primary human osteoblasts, overexpression of circ_PWWP2A can effectively inhibit dexamethasone-induced cell death and apoptosis (Hong *et al*., 2019). circ-PWWP2A is up-regulated in mouse fibrotic liver tissue and is positively correlated with HSC activation and proliferation (Liu *et al*., 2019). Similarly, MLg2908 cells were treated with TGF-β (0, 5, 10 ng/ml) and circ_PWWP2A expression was analyzed to be increased in a concentration-dependent manner. Animal experiments also found that circ_PWWP2A was also upregulated in BLM-induced rat lung tissue, suggesting that circ_PWWP2A involves the activation of lung fibroblasts and may be a pathogenic factor for IPF. After inhibiting circ_PWWP2A expression in TGF-β-induced MLg2908 cells, cell proliferation ability was reduced, which verified our speculation.

The most important function of circRNA is to play as miRNA "sponge" (Shi *et al*., 2020). The present study proved that circ_PWWP2A could adsorb miR-27b-3p. In this study, miR-27b-3p expression in MLg2908 cells induced by TGF-β was decreased, which is consistent with previous reports: for example, exosomal miR-27b derived from human umbilical cord mesenchymal stem cells can ameliorate subretinal fibrosis (Li *et al*., 2021). Also, miR-27b-3p knockout can reduce cardiac hypertrophy, fibrosis, and inflammation induced by a pathological cardiac hypertrophy model (Li *et al*., 2021). Furthermore, miR-27b-3p overexpression attenuates renal fibrosis by downregulating α-SMA and collagen III (Bai *et al*., 2021). All of the studies indicate that miR-27b-3p is a fibrosis-related gene, and its overexpression the role can beantifibrotic. Our data further described that low expression of miR-27b-3p could reverse the effect of circ_PWWP2A siRNA on TGF-β-induced mouse lung fibroblast proliferation, and circ_PWWP2A siRNA could reduce the expression of miR-27b-3p in lung tissue of IPF rats, indicating that circ_PWWP2A could adsorb miR- 27b-3p thus promoting TGF-β-induced proliferation and activating MLg2908 cells. α-SMA, collagen I and collagen III, as fibrosis-related genes are overexpressed in various tissue fibrosis, such as experimental pulmonary fibrosis (Huang *et al*., 2020), cardiac fibrosis (Zeng *et al*., 2019), liver fibrosis (Cheng *et al*., 2019), and kidney fibrosis (Zheng *et al*., 2019). Here, the expression patterns of α-SMA, collagen I, and collagen III in MLg2908 cells induced by TGF-β were increased, which were similar to the results of previous studies (Cheng *et al*., 2019; Liu *et*

al., 2017), but circ_PWWP2A siRNA can inhibit its increase. circ-PWWP2A depletion can alleviate mouse liver fibrosis, accompanied by decreased α-SMA and collagen I expression (Liu *et al*., 2019). *In vivo* experiments from the present study clarified that low expression of circ_PWWP2A can improve BLM-induced pulmonary fibrosis in rats, accompanied by decreased expression of α-SMA, collagen I, and collagen III, indicating that the inhibitory effect of circ_PWWP2A on IPF may be through the reduction of fibrosis-related genes.

miRNAs are endogenous small non-coding RNAs (Chen *et al*., 2019), which can bind to the 3'UTR of target gene mRNA (Bartel, 2009). miR-27b-3p can target the regulation of GATA3 located at 10p14 (Enciso-Mora *et al*., 2010). T cells regulate the activation of skin fibroblasts, which is in part achieved by GATA3-mediated unique tissue-restricted transcriptional program (Kalekar *et al*., 2019). GATA3 is also involved in pulmonary fibrosis development (Iturra *et al*., 2018).

On the whole, the study only discusses the mechanism from experimental tests, and future clinical experiments are required to verify our results; how GATA3 is involved in circ_PWWP2A-mediated adsorption of miR-27b-3p regulating IPF needs to be done as funds and time allow.

CONCLUSION

circ_PWWP2A expression in MLg2908 cells induced by TGF-β decreases in a concentration-dependent manner. Silencing circ_PWWP2A can inhibit the role of TGF-β in the activation and proliferation of lung fibroblasts through the miR-27b-3p/GATA3 axis, and reduce BLM-induced IPF in rats, potentially renewing therapeutic targets for IPF.

Declarations

Competing interests. The authors declare that they have no competing interests.

Ethical statement. All animal experiments were complied with the ARRIVE guidelines and performed in accordance with the National Institutes of Health Guide for the Care and Use of Laboratory Animals. The experiments were approved by the Affiliated Hospital of Inner Mongolia Medical University.

Acknowledgments. Not applicable.

Funding Statements. Not applicable.

Declaration of Conflicting Interests. Authors declared no conflict of interest.

REFERENCES

Altesha MA, Ni T, Khan A, Liu K, Zheng X (2019) Circular RNA in cardiovascular disease. *J Cell Physiol* **234**: 5588–5600. https://doi.org/10.1002/jcp.27384

Bai L, Lin Y, Xie J, Zhang Y, Wang H, Zheng D (2021) MiR-27b-3p inhibits the progression of renal fibrosis via suppressing STAT1. *Hum Cell* **34**: 383–393. https://doi.org/10.1007/s13577-020-00474-z

Bartel DP (2009) MicroRNAs: target recognition and regulatory functions. *Cell* **136**: 215–233. https://doi.org/10.1016/j.cell.2009.01.002

Chen L, Heikkinen L, Wang C, Yang Y, Sun H, Wong G (2019) Trends in the development of miRNA bioinformatics tools. *Brief Bioinform* **20**: 1836–1852. https://doi.org/10.1093/bib/bby054

Cheng Q, Li C, Yang CF, Zhong YJ, Wu D, Shi L, Chen L, Li YW, Li L (2019) Methyl ferulic acid attenuates liver fibrosis and hepatic stellate cell activation through the TGF-β1/Smad and NOX4/ROS pathways. *Chem Biol Interact* **299**: 131–139. https://doi.org/10.1016/j.cbi.2018.12.006

Cheng Z, Zhang Y, Wu S, Zhao R, Yu Y, Zhou Y, Zhou Z, Dong Y, Qiu A, Xu H, Liu Y, Zhang W, Tian T, Wu Q, Gu H, Chu M (2022) Peripheral blood circular RNA hsa_circ_0058493 as a potential novel biomarker for silicosis and idiopathic pulmonary fibrosis. *Ecotoxicol Environ Saf* **236**: 113451. https://doi.org/10.1016/j.ecoenv.2022.113451

Conserva F, Barozzino M, Pesce F, Divella C, Oranger A, Papale M, Sallustio F, Simone S, Laviola L, Giorgino F, Gallone A, Pontrelli P, Gesualdo L (2019) Urinary miRNA-27b-3p and miRNA-1228-3p correlate with the progression of Kidney Fibrosis in Diabetic Nephropathy. *Sci Rep* **9**: 11357. https://doi.org/10.1038/s41598-019-47778-1

Enciso-Mora V, Broderick P, Ma Y, Jarrett RF, Hjalgrim H, Hemminki K, van den Berg A, Olver B, Lloyd A, Dobbins SE, Lightfoot T, van Leeuwen FE, Försti A, Diepstra A, Broeks A, Vijayakrishnan J, Shield L, Lake A, Montgomery D, Roman E, Engert A, von Strandmann EP, Reiners KS, Nolte IM, Smedby KE, Adami HO, Russell NS, Glimelius B, Hamilton-Dutoit S, de Bruin M, Ryder LP, Molin D, Sorensen KM, Chang ET, Taylor M, Cooke R, Hofstra R, Westers H, van Wezel T, van Eijk R, Ashworth A, Rostgaard K, Melbye M, Swerdlow AJ, Houlston RS (2010) A genome-wide association study of Hodgkin's lymphoma identifies new susceptibility loci at 2p16.1 (REL), 8q24.21 and 10p14 (GATA3). *Nat Genet* **42**: 1126–1130. https://doi.org/10.1038/ng.696

Hewlett JC, Kropski JA, Blackwell TS (2018) Idiopathic pulmonary fibrosis: Epithelial-mesenchymal interactions and emerging therapeutic targets. *Matrix Biol* **71–72**: 112–127. https://doi.org/10.1016/j.matbio.2018.03.021

Hong H, Sun Y, Deng H, Yuan K, Chen J, Liu W, Cui Z (2019) Dysregulation of cPWWP2A-miR-579 axis mediates dexamethasone-induced cytotoxicity in human osteoblasts. *Biochem Biophys Res Commun* **517**: 491–498. https://doi.org/10.1016/j.bbrc.2019.07.095

Huang A, Zheng H, Wu Z, Chen M, Huang Y (2020) Circular RNA-protein interactions: functions, mechanisms, and identification. *Theranostics* **10**: 3503–3517. https://doi.org/10.7150/thno.42174

Huang H, Wang X, Zhang X, Wang H, Jiang W (2020) Roxadustat attenuates experimental pulmonary fibrosis *in vitro* and *in vivo*. *Toxicol Lett* **331**: 112–121. https://doi.org/10.1016/j.toxlet.2020.06.009

Iturra PA, Rojas DA, Pérez FJ, Méndez A, Ponce CA, Bonilla P, Bustamante R, Rodríguez H, Beltrán CJ, Vargas SL (2018) Progression of type 2 helper T cell-type inflammation and airway remodeling in a rodent model of naturally acquired subclinical primary pneumocystis infection. *Am J Pathol* **188**: 417–431. https://doi.org/10.1016/j.ajpath.2017.10.019

Jin J, Sun H, Shi C, Yang H, Wu Y, Li W, Dong YH, Cai L, Meng XM (2020) Circular RNA in renal diseases. *J Cell Mol Med* **24**: 6523–6533. https://doi.org/10.1111/jcmm.15295

Kalekar LA, Cohen JN, Prevel N, Sandoval PM, Mathur AN, Moreau JM, Lowe MM, Nosbaum A, Wolters PJ, Haemel A, Boin F, Rosenblum MD (2019) Regulatory T cells in skin are uniquely poised to suppress profibrotic immune responses. *Sci Immunol* **4**. https://doi.org/10.1126/sciimmunol.aaw2910

Kim MK, Lee SK, Park JH, Lee JH, Yun BH, Park JH, Seo SK, Cho S, Choi YS (2017) Ginsenoside Rg3 decreases fibrotic and invasive nature of endometriosis by modulating miRNA-27b: *in vitro* and *in vivo* studies. *Sci Rep* **7**: 17670. https://doi.org/10.1038/s41598-017-17956-0

Konigsberg IR, Borie R, Walts AD, Cardwell J, Rojas M, Metzger F, Hauck SM, Fingerlin TE, Yang IV, Schwartz DA (2021) Molecular signatures of idiopathic pulmonary fibrosis. *Am J Respir Cell Mol Biol* **65**: 430–441. https://doi.org/10.1165/rcmb.2020-0546OC

Kristensen LS, Andersen MS, Stagsted LVW, Ebbesen KK, Hansen TB, Kjems J (2019) The biogenesis, biology and characterization of circular RNAs. *Nat Rev Genet* **20**: 675–691. https://doi.org/10.1038/s41576-019-0158-7

Lei M, Zheng G, Ning Q, Zheng J, Dong D (2020) Translation and functional roles of circular RNAs in human cancer. *Mol Cancer* **19**: 30. https://doi.org/10.1186/s12943-020-1135-7

Li D, Zhang J, Liu Z, Gong Y, Zheng Z (2021) Human umbilical cord mesenchymal stem cell-derived exosomal miR-27b attenuates subretinal fibrosis via suppressing epithelial-mesenchymal transition by targeting HOXC6. *Stem Cell Res Ther* **12**: 24. https://doi.org/10.1186/s13287-020-02064-0

Li G, Shao Y, Guo HC, Zhi Y, Qiao B, Ma K, Du J, Lai YQ, Li Y (2022) MicroRNA-27b-3p down-regulates FGF1 and aggravates pathological cardiac remodelling. *Cardiovasc Res* **118**: 2139–2151. https://doi.org/10.1093/cvr/cvab248

Li J, Sun D, Pu W, Wang J, Peng Y (2020) Circular RNAs in cancer: biogenesis, function, and clinical significance. *Trends Cancer* **6**: 319–336. https://doi.org/10.1016/j.trecan.2020.01.012

Li M, Hua Q, Shao Y, Zeng H, Liu Y, Diao Q, Zhang H, Qiu M, Zhu J, Li X, Ling Y, Zhang R, Jiang Y (2020) Circular RNA circBbs9 promotes PM(2.5)-induced lung inflammation in mice *via* NLRP3 inflammasome activation. *Environ Int* **143**: 105976. https://doi.org/10.1016/j.envint.2020.105976

Li R, Wang Y, Song X, Sun W, Zhang J, Liu Y, Li H, Meng C, Zhang J, Zheng Q, Lv C (2018) Potential regulatory role of circular RNA in idiopathic pulmonary fibrosis. *Int J Mol Med* **42**: 3256–3268. https://doi.org/10.3892/ijmm.2018.3892

Li YJ, Azuma A, Usuki J, Abe S, Matsuda K, Sunazuka T, Shimizu T, Hirata Y, Inagaki H, Kawada T, Takahashi S, Kudoh S, Omura S (2006) EM703 improves bleomycin-induced pulmonary fibrosis in mice by the inhibition of TGF-beta signaling in lung fibroblasts. *Respir Res* **7**: 16. https://doi.org/10.1186/1465-9921-7-16

Liu JC, Wang F, Xie ML, Cheng ZQ, Qin Q, Chen L, Chen R (2017) Osthole inhibits the expressions of collagen I and III through Smad signaling pathway after treatment with TGF-β1 in mouse cardiac fibroblasts. *Int J Cardiol* **228**: 388–393. https://doi.org/10.1016/j.ijcard.2016.11.202

Liu W, Feng R, Li X, Li D, Zhai W (2019) TGF-β- and lipopolysaccharide-induced upregulation of circular RNA PWWP2A promotes hepatic fibrosis *via* sponging miR-203 and miR-223. *Aging (Albany NY)* **11**: 9569–9580. https://doi.org/10.18632/aging.102405

Martinez FJ, Collard HR, Pardo A, Raghu G, Richeldi L, Selman M, Swigris JJ, Taniguchi H, Wells AU (2017) Idiopathic pulmonary fibrosis. *Nat Rev Dis Primers* **3**: 17074. https://doi.org/10.1038/nrdp.2017.74

Milara J, Ballester B, Morell A, Ortiz JL, Escrivá J, Fernández E, Perez-Vizcaino F, Cogolludo A, Pastor E, Artigues E, Morcillo E, Cortijo J (2018) JAK2 mediates lung fibrosis, pulmonary vascular remodelling and hypertension in idiopathic pulmonary fibrosis: an experimental study. *Thorax* **73**: 519–529. https://doi.org/10.1136/thoraxjnl-2017-210728

Otsuka M, Shiratori M, Chiba H, Kuronuma K, Sato Y, Niitsu Y, Takahashi H (2017) Treatment of pulmonary fibrosis with siRNA against a collagen-specific chaperone HSP47 in vitamin A-coupled liposomes. *Exp Lung Res* **43**: 271–282. https://doi.org/10.1080/01902148.2017.1354946

Qiao Y, Liu L, Yin L, Xu L, Tang Z, Qi Y, Mao Z, Zhao Y, Ma X, Peng J (2019) FABP4 contributes to renal interstitial fibrosis via mediating inflammation and lipid metabolism. *Cell Death Dis* **10**: 382. https://doi.org/10.1038/s41419-019-1610-5

Sgalla G, Biffi A, Richeldi L (2016) Idiopathic pulmonary fibrosis: Diagnosis, epidemiology and natural history. *Respirology* **21**: 427–437. https://doi.org/10.1111/resp.12683

Shi Y, Jia X, Xu J (2020) The new function of circRNA: translation. *Clin Transl Oncol* **22**: 2162–2169. https://doi.org/10.1007/s12094-020-02371-1

Somogyi V, Chaudhuri N, Torrisi SE, Kahn N, Müller V, Kreuter M (2019) The therapy of idiopathic pulmonary fibrosis: what is next? *Eur Respir Rev* **28**. https://doi.org/10.1183/16000617.0021-2019

Stachowiak Z, Wojsyk-Banaszak I, Jończyk-Potoczna K, Narożna B, Langwiński W, Kycler Z, Sobkowiak P, Bręborowicz A, Szczepankiewicz A (2020) MiRNA expression profile in the airways is altered during pulmonary exacerbation in children with cystic fibrosis-a preliminary report. *J Clin Med* **9**. https://doi.org/10.3390/jcm9061887

Wakwaya Y, Brown KK (2019) Idiopathic pulmonary fibrosis: epidemiology, diagnosis and outcomes. *Am J Med Sci* **357**: 359–369. https://doi.org/10.1016/j.amjms.2019.02.013

Wolters PJ, Collard HR, Jones KD (2014) Pathogenesis of idiopathic pulmonary fibrosis. *Annu Rev Pathol* **9**: 157–179. https://doi.org/10.1146/annurev-pathol-012513-104706

Xaubet A, Ancochea J, Molina-Molina M (2017) Idiopathic pulmonary fibrosis. *Med Clin (Barc)* **148**: 170–175. https://doi.org/10.1016/j.medcli.2016.11.004

Zeng Z, Wang Q, Yang X, Ren Y, Jiao S, Zhu Q, Guo D, Xia K, Wang Y, Li C, Wang W (2019) Qishen granule attenuates cardiac fibrosis by regulating TGF-β /Smad3 and GSK-3β pathway. *Phytomedicine* **62**: 152949. https://doi.org/10.1016/j.phymed.2019.152949

Zhang T, Wei G, Millard CJ, Fischer R, Konietzny R, Kessler BM, Schwabe JWR, Brockdorff N (2018) A variant NuRD complex containing PWWP2A/B excludes MBD2/3 to regulate transcription at active genes. *Nat Commun* **9**: 3798. https://doi.org/10.1038/s41467-018-06235-9